International Journal of Fracture **73**: 301–323, 1995.

Interactions between inclusions and various types of cracks

CHYANBIN HWU[1], YIN KO LIANG[1] and WEN J. YEN[2]
[1]*Institute of Aeronautics and Astronautics, National Cheng Kung University, Tainan, Taiwan, R.O.C.*
[2]*Aeronautical Industry Development Center, Taichung, Taiwan, R.O.C.*

Received 29 July 1994; accepted 10 April 1995

Abstract. The problems of a crack inside, outside, penetrating or lying along the interface of an anisotropic elliptical inclusion are considered in this paper. Because the crack may be represented by a distribution of dislocation, integrating the analytical solutions of dislocation problems along the crack and applying the technique of numerical solution on the singular integral equation, we can obtain the general solutions to the problems of interactions between cracks and anisotropic elliptical inclusions. Since there are no analytical solutions existing for the general cases of interactions between cracks and inclusions, the comparison is made with the numerical results obtained by other methods or with the analytical results for the special cases which can be reduced from the present problems. These results show that our solutions are correct and universal.

1. Introduction

The interaction between cracks and inclusions is a typical and important problem in fracture mechanics. In the literature, discussion about the problems of the interactions between cracks and inclusions is usually restricted to isotropic materials, such as Atkinson [1] and Erdogan et al. [2], who obtained the general solutions for a crack outside an isotropic circular inclusion, and Erdogan and Gupta [3] who solved the problems of a crack inside or penetrating an isotropic circular inclusion. Also, Patton and Santare [4] studied the interaction between a crack and a rigid elliptical inclusion. As to the curvilinear interface crack problems, England [5] and Toya [6] studied a circular arc interface crack problem. Toya [7] and Herrmann [8] have dealt with the problems of a crack lying along the interface of a rigid circular inclusion. Moreover, Sih et al. [9] and Cotterell and Rice [10] have obtained the analytical solutions for a circular arc crack in homogeneous materials. However, these results can only be applied to the isotropic materials. Recently, Hwu and Liao [11] studied the problems of multi-holes, cracks and inclusions by a special boundary element, in which the materials are considered to be general anisotropic. Although their methods can be applied to study the interactions between inclusions and an outside crack, they cannot be used to study the cases of cracks located inside the inclusions, or a penetrating crack, or a curvilinear interface crack.

In this paper, we consider the interactions between inclusions and various types of cracks such as a crack located inside or outside the inclusions, a crack penetrating the inclusions, and a curvilinear crack lying along the interface between the inclusion and the matrix. With the advantage of finding the analytical solutions for a dislocation located inside, outside or on the interface of an anisotropic elliptical inclusion [12], the present problems are solved by representing the cracks as a distribution of dislocation. With this representation, the traction boundary conditions along the crack surface may be written as a singular integral equation of the Cauchy type. This singular integral equation may be solved by a special numerical technique introduced by Gerasoulis [13] with the consideration of the single-valued displacement requirement.

2. Inclusions and dislocations

Consider an anisotropic elastic elliptical inclusion embedded in an infinite matrix, and the dislocation with Burgers vector $\hat{\boldsymbol{b}}$ located at the point $(\hat{x}_1, \hat{x}_2)$ which is outside, inside or on the interface of the inclusion. If the inclusion and the matrix are assumed to be perfectly bonded along the interface, the displacements and surface tractions across the interface should be continuous. An elasticity solution satisfying the dislocation singularity and the interface continuity condition has been found in [12]. For ease of reference, the solution is listed below.

$$\left.\begin{aligned} \boldsymbol{u}_1 &= \boldsymbol{A}_1[\boldsymbol{f}_0(\zeta) + \boldsymbol{f}_1(\zeta)] + \overline{\boldsymbol{A}}_1[\overline{\boldsymbol{f}_0(\zeta)} + \overline{\boldsymbol{f}_1(\zeta)}] \\ \boldsymbol{\phi}_1 &= \boldsymbol{B}_1[\boldsymbol{f}_0(\zeta) + \boldsymbol{f}_1(\zeta)] + \overline{\boldsymbol{B}}_1[\overline{\boldsymbol{f}_0(\zeta)} + \overline{\boldsymbol{f}_1(\zeta)}] \end{aligned}\right\}, \quad \zeta \in S_1 \tag{1a}$$

and

$$\left.\begin{aligned} \boldsymbol{u}_2 &= \boldsymbol{A}_2[\boldsymbol{f}_0^*(\zeta) + \boldsymbol{f}_2(\zeta)] + \overline{\boldsymbol{A}}_2[\overline{\boldsymbol{f}_0^*(\zeta)} + \overline{\boldsymbol{f}_2(\zeta)}] \\ \boldsymbol{\phi}_2 &= \boldsymbol{B}_2[\boldsymbol{f}_0^*(\zeta) + \boldsymbol{f}_2(\zeta)] + \overline{\boldsymbol{B}}_2[\overline{\boldsymbol{f}_0^*(\zeta)} + \overline{\boldsymbol{f}_2(\zeta)}] \end{aligned}\right\}, \quad \zeta \in S_2, \tag{1b}$$

where the subscripts 1 and 2 denote, respectively, the matrix and inclusion. The over-bar represents the conjugate of a complex number. $\boldsymbol{u}$ and $\boldsymbol{\phi}$ represent, respectively, the displacements and stress functions. $\boldsymbol{A}$ and $\boldsymbol{B}$ are the material eigenvector matrices. The variable ζ is related to the complex variable $z_\alpha(= x_1 + p_\alpha x_2)$ by

$$z_\alpha = \frac{1}{2}\left\{(a - ibp_\alpha)\zeta_\alpha + (a + ibp_\alpha)\frac{1}{\zeta_\alpha}\right\}, \tag{2}$$

where $2a$ and $2b$ are the major and minor axes of the ellipse. (x_1, x_2) is a fixed rectangular coordinate system. $p_\alpha, \alpha = 1, 2, 3$, are the material eigenvalues. $\boldsymbol{f}_0$ and $\boldsymbol{f}_0^*$ represent the function associated with the singularity behavior caused by the dislocation. $\boldsymbol{f}_1$ (or $\boldsymbol{f}_2$) is the function corresponding to the field of matrix (or inclusion) and is holomorphic in region S_1 (or S_2). S_1 and S_2 denote, respectively, the regions occupied by the matrix and inclusion. The solutions provided in [12] for $\boldsymbol{f}_0$, $\boldsymbol{f}_0^*$, $\boldsymbol{f}_1$ and $\boldsymbol{f}_2$ are obtained by combining the Stroh's formalism and the method of analytical continuation. For convenience of presentation their solutions are written with all the subscripts of the variable ζ dropped, which may not be applied directly to the full domain. To have an explicit solution valid for the entire domain, we employ the translating technique introduced by Hwu [14]. The results are

(i) *A dislocation outside an elliptical inclusion*

$$
\begin{aligned}
f_0(\zeta) &= \frac{1}{2\pi i}\langle\langle \log(\zeta_\alpha - \hat{\zeta}_\alpha)\rangle\rangle \boldsymbol{B}_1^T\hat{\boldsymbol{b}},\\
f_0^*(\zeta) &= 0,\\
f_1(\zeta) &= \frac{1}{2\pi i}\sum_{k=1}^{\infty}\langle\langle \zeta_\alpha^{-k}\rangle\rangle \boldsymbol{E}_k\hat{\boldsymbol{b}}\\
&\quad + \frac{1}{2\pi i}\sum_{j=1}^{3}\langle\langle \log(\zeta_\alpha^{-1} - \bar{\hat{\zeta}}_j)\rangle\rangle \boldsymbol{B}_1^{-1}\overline{\boldsymbol{B}}_1\boldsymbol{I}_j\overline{\boldsymbol{B}}_1^T\hat{\boldsymbol{b}},\\
f_2(\zeta) &= \frac{1}{2\pi i}\sum_{k=1}^{\infty}\langle\langle \zeta_\alpha^{k} + \gamma_\alpha^k\zeta_\alpha^{-k}\rangle\rangle \boldsymbol{C}_k\hat{\boldsymbol{b}}.
\end{aligned}
\tag{3}
$$

(ii) *A dislocation inside an elliptical inclusion*

$$
\begin{aligned}
f_0(\zeta) &= \frac{1}{2\pi i}\langle\langle \log \zeta_\alpha\rangle\rangle \boldsymbol{B}_1^T\hat{\boldsymbol{b}},\\
f_0^*(\zeta) &= \frac{1}{2\pi i}\langle\langle \log(z_\alpha - \hat{z}_\alpha)\rangle\rangle \boldsymbol{B}_2^T\hat{\boldsymbol{b}},\\
f_1(\zeta) &= \frac{1}{2\pi i}\sum_{k=1}^{\infty}\langle\langle \zeta_\alpha^{-k}\rangle\rangle \boldsymbol{E}_k\hat{\boldsymbol{b}}\\
&\quad + \frac{1}{2\pi}\sum_{k=1}^{\infty}\langle\langle \zeta_\alpha^{-k}\rangle\rangle \boldsymbol{B}_1^{-1}\boldsymbol{B}_2\left\langle\left\langle \frac{-1}{k}\left(\hat{\zeta}_\alpha^k + \left(\frac{\gamma_\alpha}{\hat{\zeta}_\alpha}\right)^k\right)\right\rangle\right\rangle \boldsymbol{B}_2^T\hat{\boldsymbol{b}},\\
f_2(\zeta) &= \frac{1}{2\pi i}\sum_{k=1}^{\infty}\langle\langle \zeta_\alpha^{k} + \gamma_\alpha^{-k}\rangle\rangle \boldsymbol{C}_k\hat{\boldsymbol{b}}.
\end{aligned}
\tag{4}
$$

(iii) *A dislocation on the interface of an eliptical inclusion*

$$
\begin{aligned}
f_0(\zeta) &= \frac{1}{2\pi i}\langle\langle \log(\zeta_\alpha - \hat{\zeta}_\alpha)\rangle\rangle \boldsymbol{B}_1^T\hat{\boldsymbol{b}}\\
&\quad + \frac{1}{2\pi i}\langle\langle \log(\zeta_\alpha^{-1} - \overline{\hat{\zeta}_\alpha})\rangle\rangle \boldsymbol{Q}_1\hat{\boldsymbol{b}},\\
f_0^*(\zeta) &= \frac{1}{2\pi i}\langle\langle \log(z_\alpha - \hat{z}_\alpha)\rangle\rangle \boldsymbol{Q}_2\hat{\boldsymbol{b}},\\
f_1(\zeta) &= \frac{1}{2\pi i}\sum_{k=1}^{\infty}\langle\langle \zeta_\alpha^{-k}\rangle\rangle \boldsymbol{E}_k\hat{\boldsymbol{b}}\\
&\quad + \frac{1}{2\pi i}\sum_{k=1}^{\infty}\langle\langle \zeta_\alpha^{-k}\rangle\rangle \boldsymbol{B}_1^{-1}\boldsymbol{B}_2\left\langle\left\langle \frac{-1}{k}\left(\frac{\gamma_\alpha}{\hat{\zeta}_\alpha}\right)^k\right\rangle\right\rangle \boldsymbol{Q}_2\hat{\boldsymbol{b}},\\
f_2(\zeta) &= \frac{1}{2\pi i}\sum_{k=1}^{\infty}\langle\langle \zeta_\alpha^{k} + \gamma_\alpha^k\zeta_\alpha^{-k}\rangle\rangle \boldsymbol{C}_k\hat{\boldsymbol{b}}.
\end{aligned}
\tag{5}
$$

where

$$\begin{aligned}
E_k &= -B_1^{-1}\overline{B}_2\overline{C}_k + B_1^{-1}B_2\langle\langle\gamma_\alpha^k\rangle\rangle C_k,\\
C_k &= (G_0 - \overline{G}_k\overline{G}_0^{-1}G_k)^{-1}(T_k + \overline{G}_k\overline{G}_0^{-1}\overline{T}_k),\\
Q_1 &= (\overline{A}_2^{-1}A_1 - \overline{B}_2^{-1}B_1)^{-1}(\overline{A}_2^{-1}\overline{A}_1 - \overline{B}_2^{-1}\overline{B}_1)\overline{B}_1^T,\\
Q_2 &= (\overline{A}_1^{-1}A_2 - \overline{B}_1^{-1}B_2)^{-1}(\overline{A}_1^{-1}A_1 - \overline{B}_1^{-1}B_1)B_1^T,
\end{aligned}$$

$$T_k = \begin{cases} \dfrac{i}{k}A_1^{-T}\langle\langle\hat{\zeta}_\alpha^{-k}\rangle\rangle B_1^T, & \text{outside,}\\[2ex] (\overline{M}_1 - \overline{M}_2)\overline{A}_2\left\langle\left\langle\overline{\dfrac{-1}{k}\left(\hat{\zeta}_\alpha^k + \left(\dfrac{\gamma_\alpha}{\hat{\zeta}_\alpha}\right)^k\right)}\right\rangle\right\rangle\overline{B}_2^T, & \text{inside,}\\[2ex] (\overline{M}_1 - \overline{M}_2)\overline{A}_2\left\langle\left\langle\overline{\dfrac{-1}{k}\left(\dfrac{\gamma_\alpha}{\hat{\zeta}_\alpha}\right)^k}\right\rangle\right\rangle\overline{Q}_2, & \text{interface,}\end{cases} \tag{6a}$$

and

$$\begin{aligned}
G_0 &= (\overline{M}_1 + \overline{M}_2)A_2,\\
G_k &= (M_1 - M_2)A_2\langle\langle\gamma_\alpha^k\rangle\rangle,
\end{aligned} \tag{6b}$$

$$\gamma_\alpha = \frac{a + ibp_\alpha^*}{a - ibp_\alpha^*} \tag{6c}$$

$$I_1 = \begin{bmatrix} 1 & 0 & 0\\ 0 & 0 & 0\\ 0 & 0 & 0\end{bmatrix}, \quad I_2 = \begin{bmatrix} 0 & 0 & 0\\ 0 & 1 & 0\\ 0 & 0 & 0\end{bmatrix}, \quad I_3 = \begin{bmatrix} 0 & 0 & 0\\ 0 & 0 & 0\\ 0 & 0 & 1\end{bmatrix}. \tag{6d}$$

$M_k, k = 1, 2$, are the impedance matrices defined as $M_k = -iB_kA_k^{-1}$. Note that the solutions associated with the c_0 are ignored because the constant stress function does not produce stress, which represents the rigid body motion.

With the solution given for the displacement vector u, the strain components ϵ_{ij} can be obtained through the use of the strain-displacement relation. As for the stress components σ_{ij}, they are related to the stress function vector ϕ by

$$\sigma_{i1} = -\phi_{i,2}, \qquad \sigma_{i2} = \phi_{i,1}, \tag{7}$$

where a comma stands for differentiation. More generally, if t is the surface traction at a point on a curved boundary,

$$t = \partial\phi/\partial s, \tag{8}$$

where s is the arclength measured along the curved boundary.

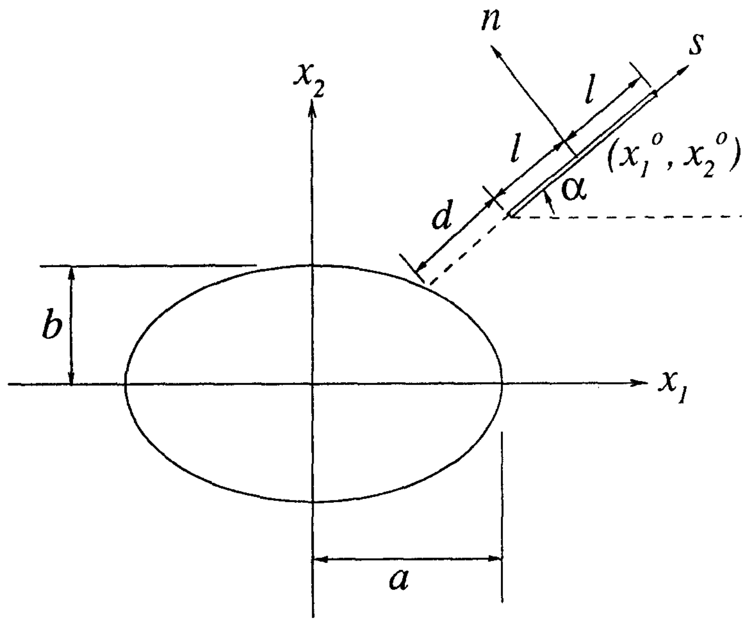

Fig. 1. The geometry of a crack outside an elliptical inclusion.

3. Inclusions and various types of cracks

In this section, we consider the interactions between inclusions and various types of cracks such as a crack located inside or outside the inclusions, a crack penetrating the inclusions, and a curvilinear crack lying along the interface between the inclusion and the matrix. By representing the cracks as a distribution of dislocation, a singular integral equation of the Cauchy type is formed, which can be solved by a special numerical technique introduced in [13].

(i) *A crack outside the inclusions*

Consider a crack located outside an elliptical anisotropic elastic inclusion subject to uniform loading at infinity, see Fig. 1. Due to the linear property, the principle of superposition can be used and the problem is represented as the sum of the following two problems: (a) an elliptical anisotropic elastic inclusion embedded in an unbounded anisotropic matrix subject to uniform loading at infinity; (b) same as the original problem except that no loading is applied at infinity and the crack surface is subject to the loading which has an opposite sense and equal magnitude as that obtained from problem (a) at the crack location.

As to problem (a), the solution has been found in [15,16], of which the stress function ϕ_1^u and ϕ_2^u can be expressed as

$$\begin{aligned}\phi_1^u &= 2\,\mathrm{Re}\{\boldsymbol{B}_1\langle\langle z_\alpha\rangle\rangle\boldsymbol{g}_1 + \boldsymbol{B}_1\langle\langle\zeta_\alpha^{-1}\rangle\rangle\boldsymbol{g}_2\},\\ \phi_2^u &= 2\,\mathrm{Re}\left\{\boldsymbol{B}_2\left\langle\left\langle\frac{2z_\alpha}{a-ibp_\alpha^*}\right\rangle\right\rangle\boldsymbol{c}_1\right\},\end{aligned} \tag{9a}$$

where

$$
\begin{aligned}
g_1 &= A_1^T t_2^\infty + B_1^T \epsilon_1^\infty, \\
g_2 &= -B_1^{-1}\left\{\overline{B}_e\overline{e}_1 + B_1\left\langle\left\langle\frac{a+ibp_\alpha}{a-ibp_\alpha}\right\rangle\right\rangle e_1 - \overline{B}_2\overline{c}_1 - B_2\langle\langle\gamma_\alpha\rangle\rangle c_1\right\}
\end{aligned}
\tag{9b}
$$

and

$$
\begin{aligned}
c_1 &= -i\{G_0 - \overline{G}_1\overline{G}_0^{-1}G_1\}^{-1}\{A_1^{-T}e_1 + \overline{G}_1\overline{G}_0\overline{A}_1^{-T}\overline{e}_1\}, \\
e_1 &= \tfrac{1}{2}\langle\langle a - ibp_\alpha\rangle\rangle g_1, \\
t_2^\infty &= \left\{\begin{matrix}\sigma_{12}^\infty \\ \sigma_{22}^\infty \\ \sigma_{32}^\infty\end{matrix}\right\}, \qquad \epsilon_1^\infty = \left\{\begin{matrix}\epsilon_{11}^\infty \\ \epsilon_{12}^\infty \\ 2\epsilon_{13}^\infty\end{matrix}\right\}.
\end{aligned}
\tag{9c}
$$

σ_{ij}^∞ and ϵ_{ij}^∞ are the uniform stresses and strains at infinity. The superscript u denotes that the solution is related to the uncracked problem.

For problem (b), we represent the crack as a distribution of dislocation. By integrating the solution shown in $(1a)_2$ and (3) for the dislocation located outside the inclusion, we have

$$
\begin{aligned}
\phi_1^d(s) = &-\frac{1}{\pi}\int_{-l}^{l} \mathrm{Re}\{iB_1\langle\langle \log(z_\alpha - \hat{z}_\alpha)\rangle\rangle B_1^T\}\beta(t)\,\mathrm{d}t \\
&-\frac{1}{\pi}\int_{-l}^{l} \mathrm{Re}\left\{iB_1\left\langle\left\langle -\log\left(1 - \frac{\gamma_\alpha}{\zeta_\alpha\hat{\zeta}_\alpha}\right)\right\rangle\right\rangle B_1^T\right\}\beta(t)\,\mathrm{d}t \\
&-\frac{1}{\pi}\int_{-l}^{l}\sum_{k=1}^{\infty} \mathrm{Re}\{iB_1\langle\langle \zeta_\alpha^{-k}\rangle\rangle E_k\}\beta(t)\,\mathrm{d}t \\
&-\frac{1}{\pi}\int_{-l}^{l}\sum_{j=1}^{3} \mathrm{Re}\{iB_1\langle\langle \log(\zeta_\alpha^{-1} - \overline{\hat{\zeta}}_j)\rangle\rangle B_1^{-1}\overline{B}_1 I_j \overline{B}_1^T\}\beta(t)\,\mathrm{d}t.
\end{aligned}
\tag{10}
$$

where the superscript d denotes that the solution is obtained by integrating the dislocation solutions. $\beta(t)$ stands for the dislocation density at point t, which is an unknown function to be determined by the boundary conditions. The variables s and t are related to z_α and $\hat{z}_\alpha$ by

$$
\begin{aligned}
z_\alpha &= (x_1^0 + p_\alpha x_2^0) + s(\cos\alpha + p_\alpha \sin\alpha), \\
\hat{z}_\alpha &= (x_1^0 + p_\alpha x_2^0) + t(\cos\alpha + p_\alpha \sin\alpha)
\end{aligned}
\tag{11}
$$

where (x_1^0, x_2^0) is the coordinate of the crack center and s (or t) denotes the distance from the crack center to point z_α (or $\hat{z}_\alpha$). The integration limits $\pm\ell$ are the ends of the crack whose length is 2ℓ.

Through the use of superposition principle, we now obtain the stress function ϕ_1 of the original problem as

$$
\phi_1 = \phi_1^u + \phi_1^d. \tag{12}
$$

If the traction $\boldsymbol{t}_n$ along the crack surface is considered to be zero, we have

$$\frac{\partial \boldsymbol{\phi}_1^d}{\partial s} = -\boldsymbol{t}_n^u, \quad \text{along the crack surface,} \tag{13}$$

where $\boldsymbol{t}_n^u$ denotes the traction along the crack location induced by problem (a) and is related to $\boldsymbol{\phi}_1^u$ by $\boldsymbol{t}_n^u = \partial \boldsymbol{\phi}_1^u / \partial s$. Substituting (10) into (13), and reconstructing the results into a form of singular integral equation, we have

$$-\frac{1}{2\pi}\int_{-l}^{l} \boldsymbol{L}_1 \boldsymbol{\beta}(t)\frac{1}{t-s}\,\mathrm{d}t + \int_{-l}^{l} \hat{\boldsymbol{K}}_1(t,s)\boldsymbol{\beta}(t)\,\mathrm{d}t = -\boldsymbol{t}_n^u(s) \tag{14a}$$

where

$$\begin{aligned} \hat{\boldsymbol{K}}_1(t,s) = & -\frac{1}{\pi}\operatorname{Re}\left\{ i\boldsymbol{B}_1 \left\langle\!\left\langle \frac{-\gamma_\alpha}{\zeta_\alpha(\zeta_\alpha\hat{\zeta}_\alpha - \gamma_\alpha)} \frac{\partial \zeta_\alpha}{\partial s} \right\rangle\!\right\rangle \boldsymbol{B}_1^T \right\} \\ & -\frac{1}{\pi}\sum_{k=1}^{\infty} \operatorname{Re}\left\{ i\boldsymbol{B}_1 \left\langle\!\left\langle -k\zeta_\alpha^{-(k+1)} \frac{\partial \zeta_\alpha}{\partial s} \right\rangle\!\right\rangle \boldsymbol{E}_k \right\} \\ & -\frac{1}{\pi}\sum_{j=1}^{3} \operatorname{Re}\left\{ i\boldsymbol{B}_1 \left\langle\!\left\langle \frac{-1}{\zeta_\alpha(1-\zeta_\alpha\bar{\hat{\zeta}}_j)} \frac{\partial \zeta_\alpha}{\partial s} \right\rangle\!\right\rangle \boldsymbol{B}_1^{-1}\overline{\boldsymbol{B}}_1 \boldsymbol{I}_j \overline{\boldsymbol{B}}_1^{-1} \right\}, \end{aligned} \tag{14b}$$

$$\frac{\partial \zeta_\alpha}{\partial s} = \frac{2\zeta_\alpha^2(\cos\alpha + p_\alpha \sin\alpha)}{(a - ibp_\alpha)\zeta_\alpha^2 - (a + ibp_\alpha)}. \tag{14c}$$

$\hat{\boldsymbol{K}}_1$ is a kernel function of the singular integral equation and is Holder-continuous along $-\ell \leqslant s \leqslant \ell$. $\boldsymbol{L}_1$ is a real matrix defined as

$$\boldsymbol{L}_1 = -2i\boldsymbol{B}_1\boldsymbol{B}_1^T. \tag{15}$$

If we nondimensionalize the variables s and t by letting $\xi = s/\ell$ and $\eta = t/\ell$, then (14a) may be rewritten as

$$-\frac{1}{2\pi}\int_{-l}^{l} \boldsymbol{L}_1 \boldsymbol{\beta}(\eta)\frac{1}{\eta-\xi}\,\mathrm{d}\eta + \int_{-l}^{l} \hat{\boldsymbol{K}}_1(\eta,\xi)\boldsymbol{\beta}(\eta)\,\mathrm{d}\eta = -\boldsymbol{t}_n^u(\xi). \tag{16}$$

The requirement of crack tip continuity will lead to the following single-valued displacement condition,

$$\int_{-1}^{1} \boldsymbol{\beta}(\eta)\,\mathrm{d}\eta = \boldsymbol{O}. \tag{17}$$

Since the order of the singularity at the crack tip is $-1/2$, it is convenient to let

$$\boldsymbol{\beta}(\eta) = \frac{\hat{\boldsymbol{\beta}}(\eta)}{\sqrt{1-\eta^2}}, \tag{18}$$

where $\hat{\beta}(\eta)$ is Holder-continuous along $-\ell \leqslant s \leqslant \ell$. Up to now, the entire problem has been reduced to finding the unknown function $\hat{\beta}(\eta)$ from the singular integral equations (16)–(18). Through the use of the numerical technique introduced in [13], which is also shown in the Appendix for completeness, the unknown dislocation density $\beta(t)$ can be determined. With $\beta(t)$ found by the traction-free boundary condition shown in (16), the single-valued displacement requirement shown in (17), and the numerical technique shown in the Appendix, the whole field solution for the stresses at point z_α can be calculated by substituting $\beta(t)$ into (9), (10) and (12). Note that the solution for ϕ_2 is not shown here for the sake of succinctness, which may easily be calculated by $\phi_2 = \phi_2^u + \phi_2^d$.

With the usual definition, the stress intensity factors may now be calculated by

$$\begin{aligned} \boldsymbol{K} = \begin{Bmatrix} K_{\rm I} \\ K_{\rm II} \\ K_{\rm III} \end{Bmatrix} &= \lim_{\xi\to\pm1}\sqrt{2\pi(\pm\xi - 1)\ell}\boldsymbol{T}\boldsymbol{t}_n(\xi) \\ &= \frac{\sqrt{\pi\ell}}{2}\boldsymbol{T}\boldsymbol{L}_1\boldsymbol{\beta}(\pm1)\,\mathrm{sgn}\,(\pm1). \end{aligned} \tag{19a}$$

where $\boldsymbol{T}$ is the transformation matrix defined as

$$\boldsymbol{T} = \begin{bmatrix} -\sin\alpha & \cos\alpha & 0 \\ \cos\alpha & \sin\alpha & 0 \\ 0 & 0 & 1 \end{bmatrix} \tag{19b}$$

and the sign function sgn(ξ) is defined as $\mathrm{sgn}(\xi) = 1$ if $\xi > 0$ and $\mathrm{sgn}(\xi) = -1$ if $\xi < 0$. It should be noted that during the derivation of (19), the following relation has been used,

$$\int_{-1}^{1}\frac{f(\eta)\,\mathrm{d}\eta}{\sqrt{1-\eta^2}(\eta-\xi)} = \frac{\pi f(\xi)}{\sqrt{\xi^2-1}}\,\mathrm{sgn}(\xi) + \text{regular terms, when } |\xi| > 1. \tag{20}$$

Moreover, the stresses $\boldsymbol{t}(\xi)$ near the crack tip ($\xi \to \pm1$) can be obtained by substituting (9), (10), (12) and (18) into (8), and using the relation shown in (20). The result is

$$\boldsymbol{t}_n(\xi) = -\tfrac{1}{2}\boldsymbol{L}_1\frac{\hat{\boldsymbol{B}}(\xi)}{\sqrt{\xi^2-1}}\,\mathrm{sgn}\,(\xi) + \text{regular terms.} \tag{21}$$

(ii) *A crack inside the inclusions*

Consider a crack located inside an elliptical anisotropic elastic inclusion subject to uniform loading at infinity, see Fig. 2. By a way similar to that described in the above subsection, one may set a singular integral equation as (14a) for the unknown dislocation density $\beta(t)$, except that now $\boldsymbol{L}_1$ should be replaced by $\boldsymbol{L}_2 = -2i\boldsymbol{B}_2\boldsymbol{B}_2^T$ and $\hat{\boldsymbol{K}}_1$ should be replaced by $\hat{\boldsymbol{K}}_2$ as

$$\begin{aligned} \hat{\boldsymbol{K}}_2(t,s) &= -\frac{1}{\pi}\sum_{k=1}^{\infty}\mathrm{Re}\left\{i\boldsymbol{B}_2\langle\langle k(\zeta_\alpha^{k-1} + \gamma_\alpha^k\zeta_\alpha^{-(k+1)})\frac{\partial\zeta_\alpha}{\partial s}\rangle\rangle\boldsymbol{C}_k\right\}, \\ \frac{\partial\zeta_\alpha}{\partial s} &= \frac{2\zeta_\alpha^2(\cos\alpha + p_\alpha^*\sin\alpha)}{(a - ibp_\alpha^*)\zeta_\alpha^2 - (a + ibp_\alpha^*)}. \end{aligned} \tag{22}$$

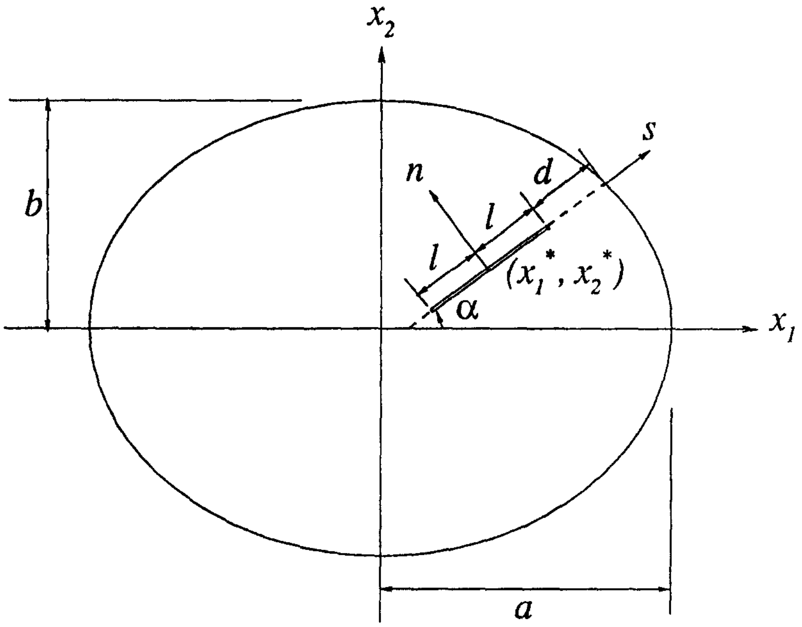

Fig. 2. The geometry of a crack inside an elliptical inclusion.

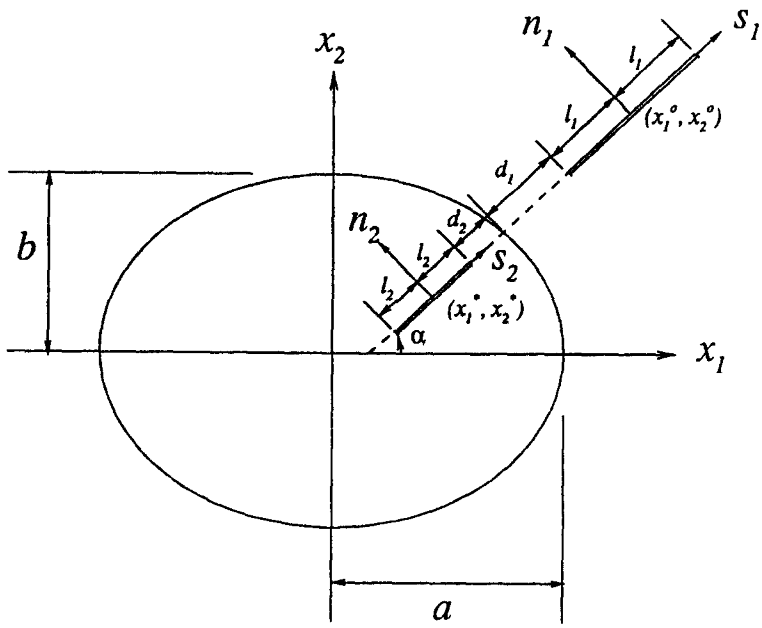

Fig. 3. The geometry of two cracks located simultaneously outside and inside an elliptical inclusion.

The formula for the stress intensity factors will also be the same as (19a) except that $\boldsymbol{L}_1$ is replaced by $\boldsymbol{L}_2$.

(iii) *A crack penetrating the inclusions*

To consider the penetrating cracks, we first deal with the case that two cracks locate simultaneously inside and outside the inclusions, Fig. 3. By a way similar to that described in subsection (i), we now obtain the singular integral equation as

$$\begin{aligned}
&-\frac{1}{2\pi}\int_{-l_1}^{l-1} \boldsymbol{L}_1\boldsymbol{\beta}_1(t_1)\frac{1}{t_1-s_1}\,\mathrm{d}t_1+\int_{-l_1}^{l_1}\hat{\boldsymbol{K}}_{11}(t_1,s_1)\boldsymbol{\beta}_1(t_1)\,\mathrm{d}t_1\\
&\quad+\int_{-l_2}^{l_2}\hat{\boldsymbol{K}}_{12}(t_2,s_1)\boldsymbol{\beta}_2(t_2)\,\mathrm{d}t_2=-\boldsymbol{t}_{1n}^u,\\
&-\frac{1}{2\pi}\int_{-l_2}^{l_2} \boldsymbol{L}_2\boldsymbol{\beta}_2(t_2)\frac{1}{t_2-s_2}\,\mathrm{d}t_2+\int_{-l_2}^{l_2}\hat{\boldsymbol{K}}_{22}(t_2,s_2)\boldsymbol{\beta}_2(t_2)\dot{\mathrm{d}}t_2\\
&\quad+\int_{-l_1}^{l_1}\hat{\boldsymbol{K}}_{21}(t_1,s_2)\boldsymbol{\beta}_1(t_1)\,\mathrm{d}t_1=-\boldsymbol{t}_{2n}^u,
\end{aligned}\tag{23a}$$

where

$$\begin{aligned}
\hat{\boldsymbol{K}}_{11}(t_1,s_1) &= -\frac{1}{\pi}\mathrm{Re}\left\{i\boldsymbol{B}_1\left\langle\left\langle\frac{-\gamma_\alpha}{\zeta_\alpha(\zeta_\alpha\hat{\zeta}_\alpha-\gamma_\alpha)}\frac{\partial\zeta_\alpha}{\partial s_1}\right\rangle\right\rangle\boldsymbol{B}_1^T\right\}\\
&\quad-\frac{1}{\pi}\sum_{k=1}^{\infty}\mathrm{Re}\left\{i\boldsymbol{B}_1\left\langle\left\langle-k\zeta_\alpha^{-(k+1)}\frac{\partial\zeta_\alpha}{\partial s_1}\right\rangle\right\rangle\boldsymbol{E}_k\right\}\\
&\quad-\frac{1}{\pi}\sum_{j=1}^{3}\mathrm{Re}\left\{i\boldsymbol{B}_1\left\langle\left\langle\frac{-1}{\zeta_\alpha(1-\zeta_\alpha\bar{\hat{\zeta}}_j)}\frac{\partial\zeta_\alpha}{\partial s_1}\right\rangle\right\rangle\boldsymbol{B}_1^{-1}\overline{\boldsymbol{B}}_1\boldsymbol{I}_j\overline{\boldsymbol{B}}_1^{-1}\right\},\\
\hat{\boldsymbol{K}}_{12}(t_2,s_1) &= -\frac{1}{\pi}\mathrm{Re}\left\{i\boldsymbol{B}_1\left\langle\left\langle\frac{1}{\zeta_\alpha}\frac{\partial\zeta_\alpha}{\partial s_1}\right\rangle\right\rangle\boldsymbol{B}_1^T\right\}\\
&\quad-\frac{1}{\pi}\sum_{k=1}^{\infty}\mathrm{Re}\left\{i\boldsymbol{B}_1\left\langle\left\langle-k\zeta_\alpha^{-(k+1)}\frac{\partial\zeta_\alpha}{\partial s_1}\right\rangle\right\rangle\boldsymbol{E}_k\right\}\\
&\quad-\frac{1}{\pi}\sum_{k=1}^{\infty}\mathrm{Re}\left\{i\boldsymbol{B}_1\left\langle\left\langle-k\zeta_\alpha^{-(k+1)}\frac{\partial\zeta_\alpha}{\partial s_1}\right\rangle\right\rangle\boldsymbol{B}_1^{-1}\boldsymbol{B}_2\right.\\
&\quad\left.\times\left\langle\left\langle\frac{-1}{k}\left(\hat{\zeta}_\alpha^k+\left(\frac{\gamma_\alpha}{\hat{\zeta}_\alpha}\right)^k\right)\right\rangle\right\rangle\boldsymbol{B}_2^T\right\}
\end{aligned}\tag{23b}$$

and

$$\begin{aligned}
\hat{\boldsymbol{K}}_{22}(t_2,s_2) &= -\frac{1}{\pi}\sum_{k=1}^{\infty}\mathrm{Re}\left\{i\boldsymbol{B}_2\left\langle\left\langle k(\zeta_\alpha^{k-1}+\gamma_\alpha^k\zeta_\alpha^{-(k+1)})\frac{\partial\zeta_\alpha}{\partial s_2}\right\rangle\right\rangle\boldsymbol{C}_k\right\},\\
\hat{\boldsymbol{K}}_{21}(t_1,s_2) &= -\frac{1}{\pi}\sum_{k=1}^{\infty}\mathrm{Re}\left\{i\boldsymbol{B}_2\left\langle\left\langle k(\zeta_\alpha^{k-1}+\gamma_\alpha^k\zeta_\alpha^{-(k+1)})\frac{\partial\zeta_\alpha}{\partial s_2}\right\rangle\right\rangle\boldsymbol{C}_k\right\}
\end{aligned}\tag{23c}$$

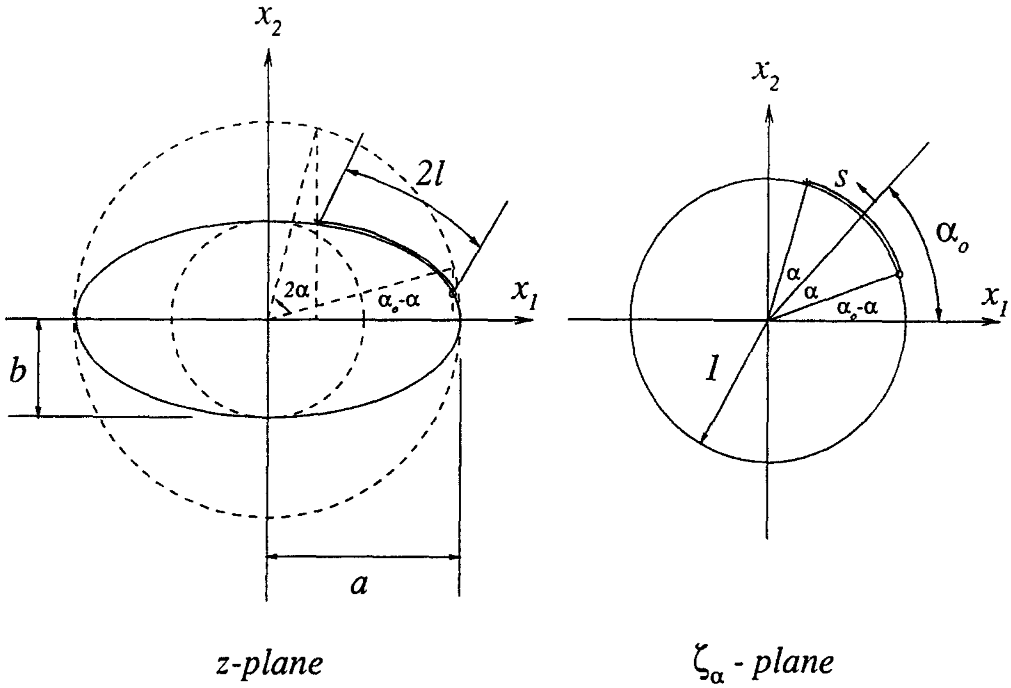

Fig. 4. The geometry of a curvilinear crack lying along the interface of an elliptical inclusion and the relation between z-plane and ζ_α-plane.

$\beta_1(t)$ and $\beta_2(t)$ denote, respectively, the dislocation density along the cracks outside and inside the inclusions. They will be determined by the set of singular integral equations shown in (23) and the single-valuedness requirement for both of the cracks. The stress intensity factors for both of the cracks can be calculated by

$$\boldsymbol{K}_i = \frac{\sqrt{\pi \ell_i}}{2} \boldsymbol{T}\boldsymbol{L}_i \hat{\boldsymbol{\beta}}_i(\pm 1)\,\mathrm{sgn}\,(\pm 1), \quad i = 1, 2, \tag{24}$$

where the subscripts 1 and 2 denote the values outside and inside the inclusions.

With the above results, by letting the distance between these two cracks approach to zero, we may approximate the condition of penetrating cracks. The detailed discussion of this approximation is shown in the next section.

(iv) *A curvilinear crack lying along the interface*

Consider a curvilinear crack lying along the interface between the inclusions and the matrices, see Fig. 4. In the same manner as the problem discussed in subsection (i) for a crack outside the inclusions, we represent the problem as the sum of two problems. One is a uncracked problem of which the solution is given in (9), the other is a loaded crack problem of which the crack is represented as a distribution of dislocation. The difference is that the dislocation is lying on the curvilinear interface. By integrating the solutions given in (5) along the elliptical interface, we have

$$\begin{aligned}\phi_2^d(s) = & -\frac{1}{\pi}\int_{-\alpha}^{\alpha} \mathrm{Re}\{i\boldsymbol{B}_2\langle\langle \log(\zeta_\alpha - \hat{\zeta}_\alpha)\rangle\rangle\boldsymbol{Q}_2\}\beta(t)\,\mathrm{d}t \\ & -\frac{1}{\pi}\int_{-\alpha}^{\alpha} \mathrm{Re}\left\{i\boldsymbol{B}_2\left\langle\left\langle \log\left(1 - \frac{\gamma_\alpha}{\zeta_\alpha\hat{\zeta}_\alpha}\right)\right\rangle\right\rangle\boldsymbol{Q}_2\right\}\beta(t)\,\mathrm{d}t \\ & -\frac{1}{\pi}\int_{-\alpha}^{\alpha}\sum_{k=1}^{\infty} \mathrm{Re}\{i\boldsymbol{B}_2\langle\langle \zeta_\alpha^k + \gamma_\alpha^k\zeta_\alpha^{-k}\rangle\rangle\boldsymbol{C}_k\}\beta(t)\,\mathrm{d}t.\end{aligned} \tag{25}$$

In the above, only the stress function ϕ_2 for the inclusions are shown, since in the following discussion about the boundary conditions of the traction-free interface crack either of ϕ_1 or ϕ_2 can be used. We choose ϕ_2 for its relative simplicity. After determining the dislocation density from the boundary conditions and the single-valued requirement, the calculation of the whole field solutions should include both ϕ_1 and ϕ_2 depending upon the point considered.

In (25), s (or t) denote the angle from the crack center to point z_α (or $\hat{z}_\alpha$) in ζ_α-domain. The integration limits $\pm\alpha$ are the ends of the cracks whose angle is 2α (in ζ_α-domain). It should be noted that use of the values in ζ_α-domain is just for the convenience of mathematical manipulation. For engineering applications, one should know the geometric relations between z-domain and ζ_α-domain, which are (also see Fig. 4)

$$z_\alpha = x_1 + p_\alpha^* x_2 = a\cos(\alpha_0 + s) + bp_\alpha^*\sin(\alpha_0 + s), \tag{26}$$

where α_0 is the angle of the crack center from the x_1-axis in ζ_α-domain.

By following the steps stated in (12)–(14), and carefully differentiating ϕ_2^d along the curvilinear crack boundary (one may refer to [17] for detailed derivation about differentiation), we obtain

$$-\frac{1}{2\pi}\int_{-\alpha}^{\alpha}\frac{2\,\mathrm{Re}(i\boldsymbol{B}_2\boldsymbol{Q}_2)}{\rho(s)}\frac{1}{t-s}\beta(t)\,\mathrm{d}t + \int_{-\alpha}^{\alpha}\hat{\boldsymbol{K}}_f(t,s)\beta(t)\,\mathrm{d}t = -\boldsymbol{t}_n^u \tag{27a}$$

where

$$\begin{aligned}\hat{\boldsymbol{K}}_f(t,s) = & -\frac{1}{\pi}\mathrm{Re}\left\{-i\boldsymbol{B}_2\frac{\boldsymbol{Q}_2}{2\rho(s)}\left(\frac{2}{t-s} - \cot\frac{t-s}{2}\right)\right\} \\ & -\frac{1}{\pi}\mathrm{Re}\left\{i\boldsymbol{B}_2\left\langle\left\langle\frac{-i}{\rho(s)}\frac{\gamma_\alpha}{e^{i(\alpha_0+s)}e^{i(\alpha_0+t)} - \gamma_\alpha}\right\rangle\right\rangle\boldsymbol{Q}_2\right\} \\ & -\frac{1}{\pi}\mathrm{Re}\left\{i\boldsymbol{B}_2\left\langle\left\langle\frac{-ik}{\rho(s)}(e^{ik(\alpha_0+s)} - \gamma_\alpha e^{-ik(\alpha_0+s)})\right\rangle\right\rangle\boldsymbol{C}_k\right\},\end{aligned} \tag{27b}$$

and

$$\rho^2(s) = a^2\sin^2(\alpha_0 + s) + b^2\cos^2(\alpha_0 + s). \tag{27c}$$

Nondimensionalization by $\xi = s/\alpha$ and $\eta = t/\alpha$ for (27a) leads to

$$-\frac{1}{2\pi}\int_{-1}^{1}\boldsymbol{L}_f\beta(\eta)\frac{1}{\eta-\xi}\,\mathrm{d}\eta + \int_{-1}^{1}\hat{\boldsymbol{K}}_f(\eta,\xi)\beta(\eta)\,\mathrm{d}\eta = -\boldsymbol{t}_n^u, \tag{28a}$$

where

$$L_f = \frac{2}{\rho(\xi)}\mathrm{Re}(i\boldsymbol{B}_2\boldsymbol{Q}_2). \tag{28b}$$

The single-valued displacement requirement can also be written in the same form as (17).

At first glance, the kernel function given in (27b) seems to be singular for the presence of the term $\frac{2}{t-s}$. However, by expanding the cot $\frac{t-s}{2}$ into the series expression as

$$\cot\frac{t-s}{2} = \frac{2}{t-s} - \frac{t-s}{6} - \frac{(t-s)^3}{360} - \cdots, \quad \left|\frac{t-s}{2}\right| < \pi. \tag{29}$$

we see that $\hat{\boldsymbol{K}}_f$ will still be Holder-continuous along the curvilinear crack.

Till now, we have set the traction-free boundary conditions by the singular integral equation shown in (27), and the single-valued displacement requirement shown in (17). Like those stated in subsection (i), the next thing should be finding a numerical technique to solve the unknown dislocation density $\beta(t)$. The technique shown in the Appendix is valid for $\beta(t)$ to be singular in the order of $-1/2$. It is well known that the singularity order of the interface crack is $-1/2 + i\epsilon$ where ϵ is the oscillation index depending on the materials of the matrices and the inclusions. To overcome this problem, it looks like a new numerical technique should be developed. However, unlike singularity, oscillation will not cause numerical overflow. Moreover, by the experimental study of Hwu et al. [18], we see that the oscillation index ϵ is usually very small which means that the range of its influence is limited. The values of the bimaterial stress intensity factors considering the oscillation effects are also very close to those of the conventional stress intensity factors considering only the $-1/2$ singularity. With the above reasons, the numerical technique shown in the Appendix is still employed, and the stress intensity factors calculated by (19) are still used except now $\boldsymbol{L}_1$ is replaced by $\boldsymbol{L}_f$ and ℓ is replaced by α.

4. Results and discussion

Since there are no analytical solutions existing for the general cases of interactions between cracks and inclusions, in the following the comparison is made with the numerical results obtained by the other methods or with the analytical results for the special cases which can be reduced from the present problems. Following is the discussion of the comparison of each type of crack considered in this paper.

(i) *A crack outside the inclusions*

To verify our results, we first consider the degenerate cases where both of the inclusions and the matrices are isotropic. Table 1 shows that our results for the stress intensity factors are almost the same as those presented by Erdogan et al. [2], in which the material properties are chosen to be $G_2/G_1 = 23, \nu_1 = 0.35, \nu_2 = 0.3$; the geometry is represented by $b/a = 1, \ell/a = 0.5, \alpha = 0°$ and the uniform loading σ_{22}^{∞} is applied at infinity. The difference is that our solutions are suitable for general anisotropic media and the shape of the inclusions is an ellipse which includes circle and line, however, those presented by [2] are valid only for the isotropic media and circular inclusions

Another comparison is made with Patton and Santare [4] for rigid elliptical inclusions, in which the Poisson's ratio ν of both inclusions and matrices is chosen to be 0.25, and

Table 1. The stress intensity factor for a crack outside an isotropic circular inclusion ($K^* = K/\sqrt{\pi l}\sigma_{22}^{\infty}$)

$(x_1^0/a, x_2^0/a)$	$K_I^*(-l)$ present	$K_I^*(-l)$ Erdogan*	$K_{II}^*(-l)$ present	$K_{II}^*(-l)$ Erdogan*	$K_I^*(l)$ present	$K_I^*(l)$ Erdogan*	$K_{II}^*(l)$ present	$K_{II}^*(l)$ Erdogan*
(1.4,0.5)	0.496	0.483	0.164	0.167	0.783	0.781	−0.064	0.002
(1.5,0.5)	0.613	0.613	0.061	0.057	0.817	0.817	−0.067	−0.005
(1.75,0.5)	0.750	0.752	−0.041	−0.047	0.878	0.878	−0.062	−0.012
(2.0,0.5)	0.834	0.833	−0.062	−0.068	0.915	0.914	−0.052	−0.012
(3.0,0.5)	0.956	0.952	−0.035	−0.041	0.973	0.970	−0.024	−0.006
(4.0,0.5)	0.982	0.980	−0.016	−0.021	0.987	0.985	−0.012	−0.002

(* Erdogan et al. [2])

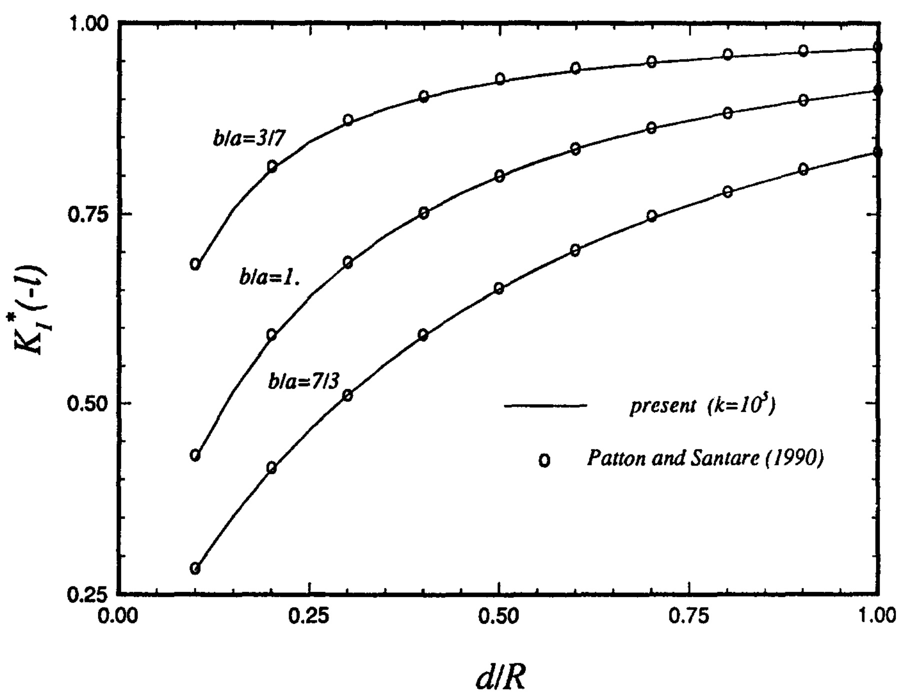

Fig. 5. The stress intensity factor for a crack outside an anisotropic circular inclusion ($\ell/R = 0.5, \alpha = 0°, R = (a+b)/2$).

the hardness index $k(= E_2/E_1)$ is chosen to be 10^5 to represent rigid inclusions. Figure 5 shows that our results are exactly the same as those presented in [4] for the cases of rigid inclusions.

The next example is for the general anisotropic elliptical inclusions. Consider a unidirectional composite laminate with the matrix material properties given by

$$E_1 = 1.2\,\text{GPa}, \quad E_2 = 0.6\,\text{GPa}, \quad G_{12} = 0.07\,\text{GPa}, \quad \nu_{12} = 0.071,$$

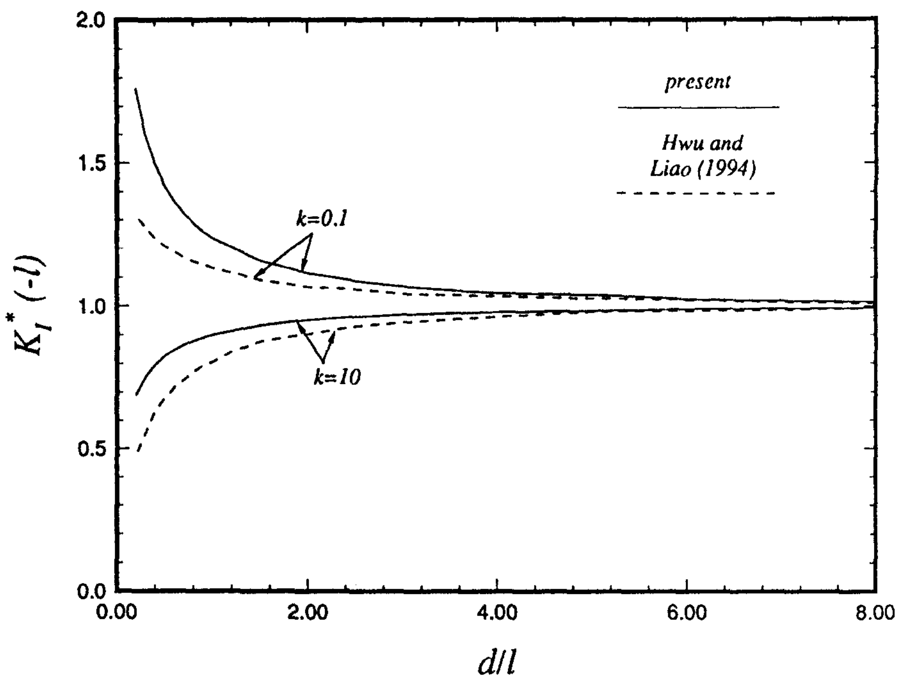

Fig. 6. The stress intensity factor for a crack outside an anisotropic circular inclusion ($K_I^* = K_I/\sqrt{\pi l}\sigma_{22}^{\infty}$, $[0°]_s$ laminates).

and the inclusion is chosen to be

$$\frac{(E_i)_2}{(E_i)_1} = \frac{(G_{ij})_2}{(G_{ij})_1} = k, \qquad i, j = 1, 2,$$

where k is the hardness index whose value is given in the figure. The geometry properties used in our example are $b/a = 1, \ell/a = 0.5, \alpha = 0°$, and d denotes the distance from the crack tip to the inclusion boundary. From Fig. 6, we see that a little discrepancy occurs when the distance $d/\ell \leqslant 5$. The inaccuracy should come from [11] since they said that their solution will not be good enough when the crack comes closer to the inclusions. The reason that their approximation fails is due to the subregion technique used in their boundary element formulation, which may cause boundary effects when the distance between the cracks and the inclusions is too short. However, in our formulation, we do not have this problem since the convergency when the dislocation is near the interface has been proved by Yen et al. [12].

(ii) *A crack inside the inclusion*

In this case, we use the same material, geometry and loading conditions as in Table 1 except $G_2/G_1 = 3, \nu_1 = 0.3$ and now the crack is located inside the inclusions. After actual numerical calculation, the results for the stress intensity factors can be shown to be identical to those presented in [3].

(iii) *A crack penetrating the inclusions*

We first check the case when two cracks locate simultaneously outside and inside the inclusions. By using the same material, geometry and loading conditions as in Table 1 except $G_2/G_1 = 23.077, \ell_1/a = 0.5, \ell_2/a = 0.25$ and now we have two cracks instead of one, the results for the stress intensity factors in Fig. 7 can be shown to be identical to those presented

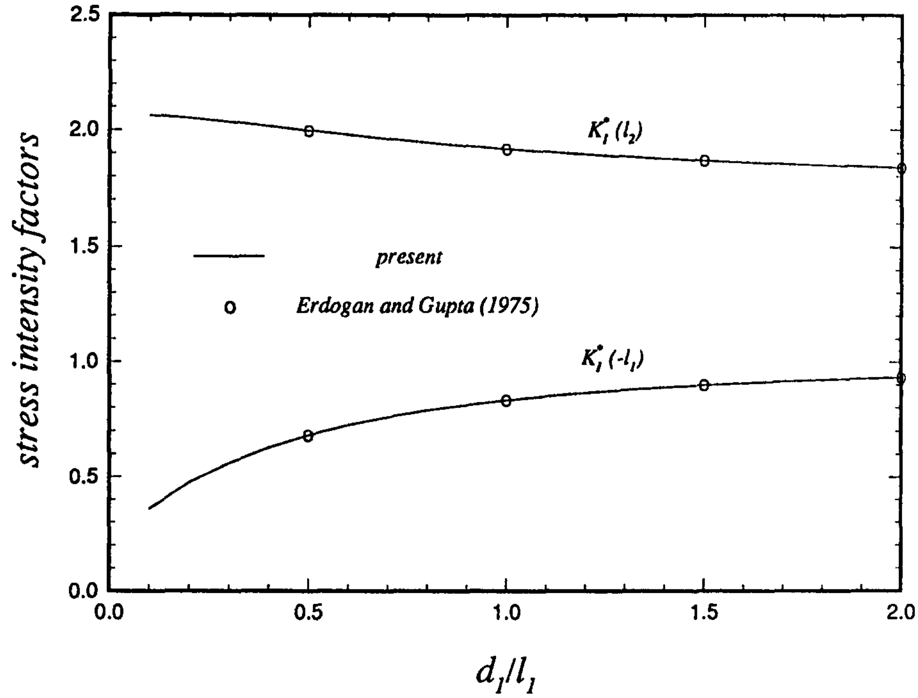

Fig. 7. The stress intensity factor for two cracks located simultaneously outside and inside an isotropic circular inclusion ($K_I^*(-l_1) = K_I(-l_1)/\sqrt{\pi l_1}\sigma_{22}^{\infty}, K_I^*(l_2) = K_I(l_2)/\sqrt{\pi l_2}\sigma_{22}^{\infty}$).

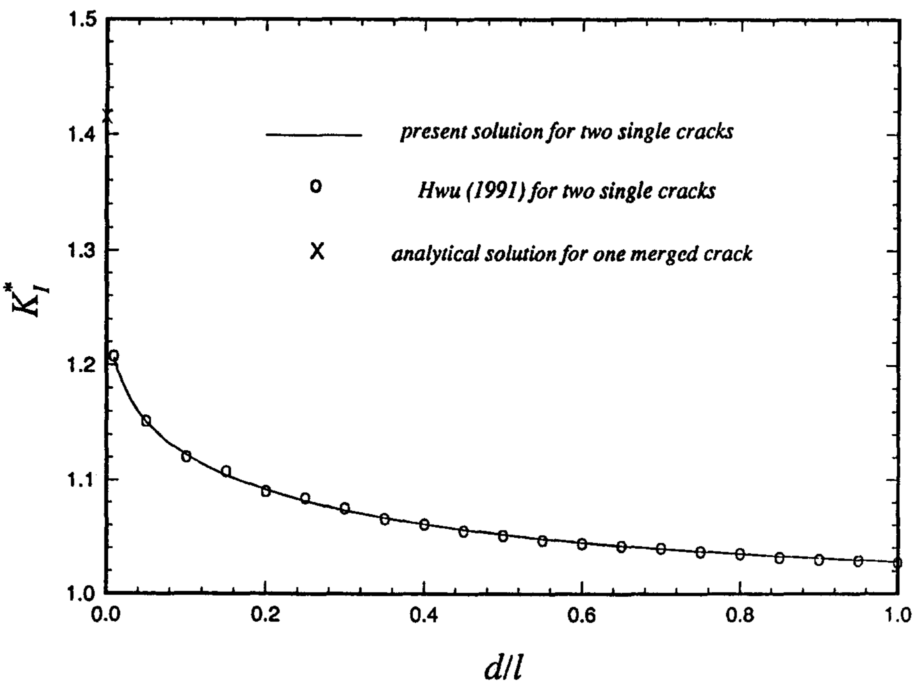

Fig. 8. The stress intensity factor for two collinear cracks in homogeneous anisotropic materials ($K_I^* = K_I/\sqrt{\pi l_1}\sigma_{22}^{\infty}$).

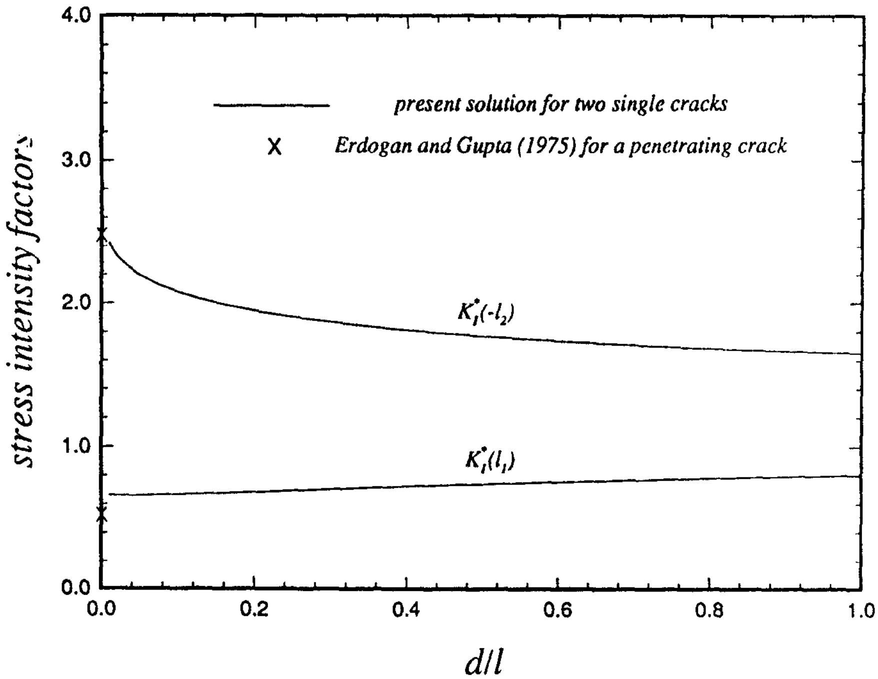

Fig. 9. The stress intensity factor for two cracks located simultaneously outside and inside the inclusion ($K_I^*(l_1) = K_I(l_1)/\sqrt{\pi l_1}\sigma_{22}^\infty$, $K_I^*(-l_2) = K_I(-l_2)/\sqrt{\pi l_2}\sigma_{22}^\infty$).

in [3]. To approximate the condition of penetrating cracks, we let the distance between these two cracks approach zero. Figures 8 and 9 show the study of the stress intensity factors when the distance between two cracks is approaching zero. The same material properties of the matrices and the inclusions have been used in Fig. 8 to simulate the case of homogeneous anisotropic media containing two collinear cracks, whose analytical solutions have been shown in [19]. The important thing in the discussion of penetrating cracks is the correctness when the distance d is made to be zero. From Fig. 8 we see that although our results for two collinear cracks are almost identical to the analytical results given in [19], when $d \to 0$ it is still difficult to get the exact result for a merged (penetrating) crack. The error is about $(1.414 - 1.206)/1.414 \times 100\% = 14.7\%$ when we use $d/\ell = 0.01$. A similar situation is shown in Fig. 9 (the material, geometry and loading conditions are the same as in Fig. 7 except $\ell_1/a = \ell_2/a = 0.25$), in which the error is about 1.77 percent for $K_I^*(-\ell_2)$ and 29.4 percent for $K_I^*(\ell_1)$. The reason for this inaccuracy may come from the following facts. Two single cracks with infinitesimal spacing will let the inner tip stress intensity factor approach infinity which is the thrust for emerging two cracks into one larger crack. The closer the distance, the larger the inner tip stress intensity factors, which is very different from the penetrating crack because the stress intensity factor for the penetrating crack at this portion (the inner tips of two single cracks) is zero since no crack tip exists at the inner portion of the penetrating cracks.

(iv) *A curvilinear crack lying along the interface*

To verify our results, we consider the simplest case where the matrices and inclusions are composed of the same materials. That is, we consider a curved crack with radius a located in a homogeneous medium subject to uniform loading σ_{11}^∞ at infinity. Figure 10 shows that our solutions for the stress intensity factors of curved cracks in homogeneous isotropic materials are exactly the same as the analytical solutions presented in [20]. As expected these factors are independent of the material properties for the isotropic media. However, it is quite surprising that they do depend upon the material properties for general anisotropic media.

Another comparison is made with Perlman and Sih [21] for the curvilinear interface cracks between two dissimilar isotropic media subject to uniform loading σ_{11}^{∞} at infinity, in which the Poisson's ratio of both inclusions and matrices is chosen to be 0.25, and the hardness index k is given in the figure. From Fig. 11, we see that our solutions are almost the same as those presented in [21] for this simplified case

5. Conclusions

The general solutions of the interactions between various cracks and anisotropic elliptical inclusions are provided in this paper by applying the analytical solutions of the dislocation problems and the technique of numerical solution on the singular integral equation. Because the general solutions of the interactions between various cracks and anisotropic elliptical inclusions cannot be found in the literature, we compare the numerical results of some special cases to prove our results are correct and universal. Due to the series terms given in the analytical solutions for the dislocation problems (of which the convergency has been studied in [12]), the efficiency of the present method will be reduced when the crack tip is near the interface. Moreover, owing to the inherited difference between two single cracks with infinitesimal spacing and one penetrating crack, our results for penetrating cracks are just approximate.

Appendix

Using the analytical solutions of the interactions between dislocations and inclusions to treat the problems of the interactions between cracks and inclusions, we will always obtain a singular integral equation as

$$\frac{-\boldsymbol{L}}{2\pi}\int_{-1}^{1}\frac{\boldsymbol{\beta}(\eta)}{\eta-\xi}\,\mathrm{d}\eta+\int_{-1}^{1}\hat{\boldsymbol{K}}(\eta,\xi)\boldsymbol{\beta}(\eta)\,\mathrm{d}\eta=\boldsymbol{f}(\xi),\quad |\xi|<1 \tag{A.1}$$

and another equation from the single-valued condition

$$\int_{-1}^{1}\boldsymbol{\beta}(\eta)\,\mathrm{d}\eta=\boldsymbol{A}, \tag{A.2}$$

where $\boldsymbol{\beta}(\eta)$ is the unknown function, $\hat{\boldsymbol{K}}(\eta,\xi)$ is the kernel function which is bounded in $[-1,1]$, $\boldsymbol{f}(\xi)$ is a known input function which is also bounded in $[-1,1]$, and $\boldsymbol{L}$ and $\boldsymbol{A}$ are constants. $\boldsymbol{A}$ is usually equal to zero for single-valued condition. Because the singular order of $\boldsymbol{\beta}(\eta)$ in this paper is $\frac{-1}{2}$, $\boldsymbol{\beta}(\eta)$ can be expressed as

$$\begin{aligned}\boldsymbol{\beta}(\eta) &= w(\eta)\hat{\boldsymbol{\beta}}(\eta),\\ w(\eta) &= \frac{1}{\sqrt{1-\eta^2}},\end{aligned} \tag{A.3}$$

where $\hat{\boldsymbol{\beta}}(\eta)$ is a continuous function in $[-1,1]$.

From the paper of Gerasoulis [13], we can divide the interval $[-1,1]$ into $2n$ parts (usually in $2n$ equal parts). Define $\eta_0=-1, \eta_i=\eta_{i-1}+h_i, i=1,2,\ldots,2n$ where h_i is the length of

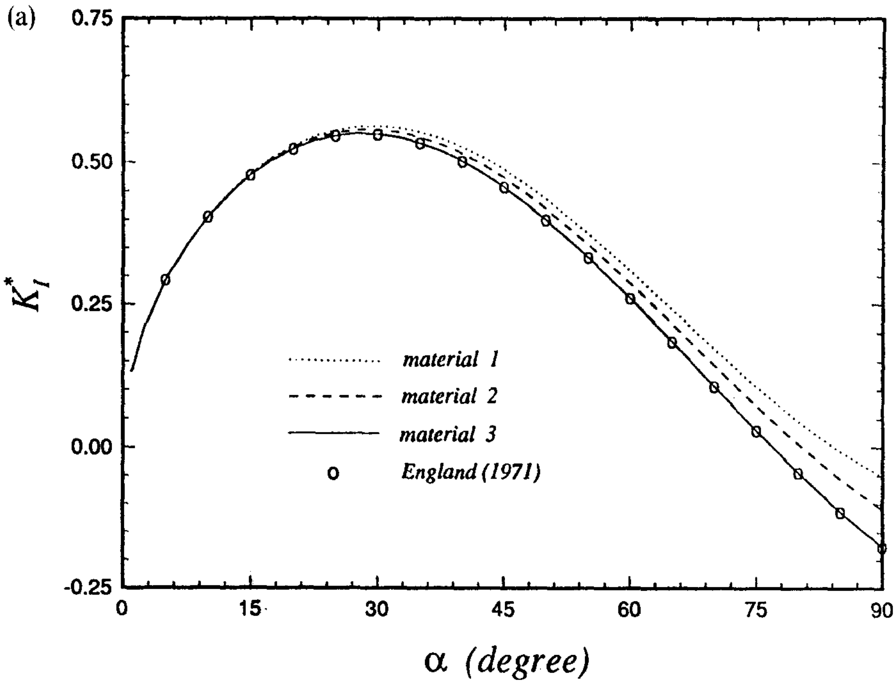

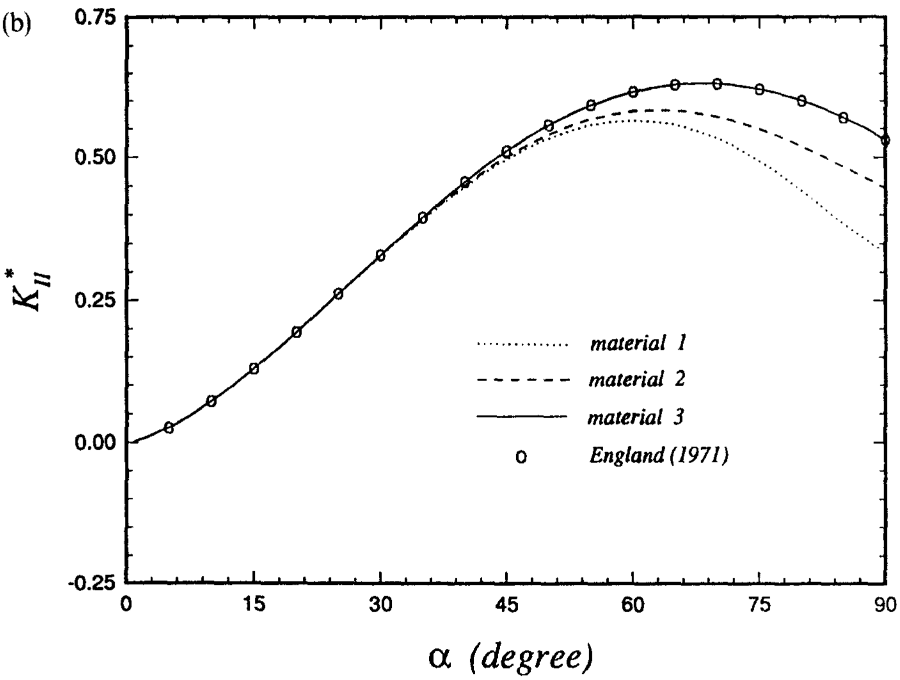

Fig. 10. The stress intensity factor for a curvilinear crack in homogeneous media ($K_I^* = K_I/\sigma_{11}^{\infty}\sqrt{\pi a}$, $K_{II}^* = K_{II}/\sigma_{11}^{\infty}\sqrt{\pi a}$; material 1: $E_1 = 133.8\,\text{GPa}$, $E_2 = E_3 = 9.58\,\text{GPa}$, $G_{12} = G_{13} = G_{23} = 4.8\,\text{GPa}$, $\nu_{12} = \nu_{13} = \nu_{23} = 0.28$; material 2: $E_1 = 48.27\,\text{GPa}$, $E_2 = E_3 = 17.24\,\text{GPa}$, $G_{12} = G_{13} = G_{23} = 6.9\,\text{GPa}$, $\nu_{12} = \nu_{13} = \nu_{23} = 0.28$; material 3: isotropic materials).

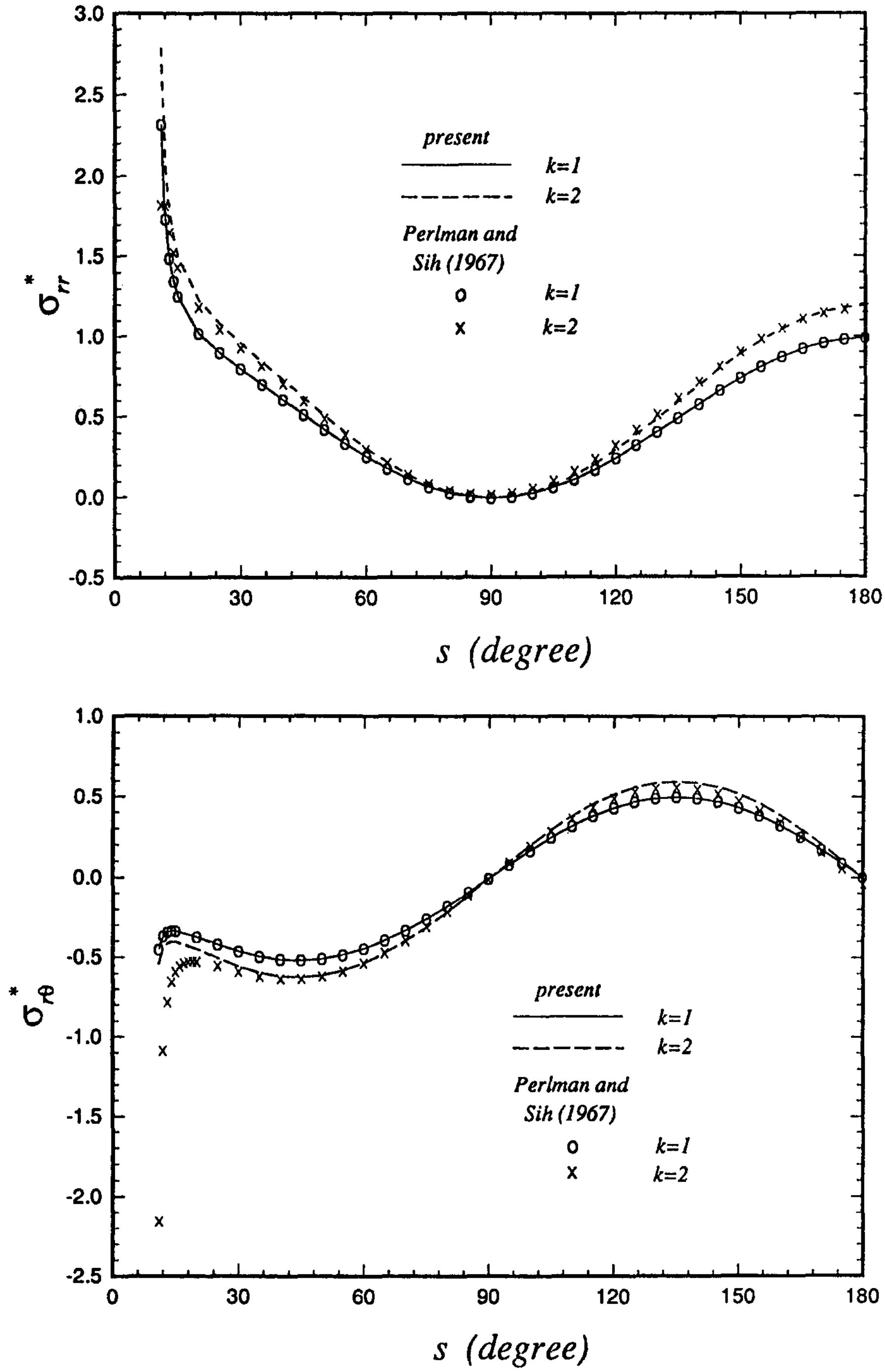

Fig. 11. The stresses along the curvilinear interface between the inclusion and matrices ($\alpha = 0°, \sigma^*_{ij} = \sigma_{ij}/\sigma_1^\infty$).

the ith interval. Applying the Lagrange interpolation formula for three points to approximate $\beta(\eta)$ in (A.3), $\hat{\boldsymbol{K}}(\eta, \xi)\hat{\beta}(\eta)$ and $\hat{\beta}(\eta)$ can be expressed as

$$\begin{aligned} \hat{\boldsymbol{K}}(\eta, \xi)\hat{\beta}(\eta) &= \sum_{i=2k-2}^{2k} l_i(\eta)\hat{\boldsymbol{K}}(\eta_i, \xi)\hat{\beta}(\eta_i), \\ \hat{\beta}(\eta) &= \sum_{i=2k-2}^{2k} l_i(\eta)\hat{\beta}(\eta_i), \end{aligned} \qquad \text{(A.4a)}$$

and

$$l_i(\eta) = \prod_{\substack{j=2k-2 \\ j\neq i}}^{2k} \left(\frac{\eta - \eta_j}{\eta_i - \eta_j}\right), \tag{A.4b}$$

for each $k = 1, 2, \ldots, n$ and $\eta_{2k-2} \leqslant \eta \leqslant \eta_{2k}$.

From (A.4a) and (A.4b), we find that (A.1) and (A.2) are approximated by

$$\begin{aligned} f(\xi) = & -\frac{\boldsymbol{L}}{2\pi}\sum_{k=1}^{n}\left\{\sum_{i=2k-2}^{2k}\beta(\eta_i)\left[\int_{\eta_{2k-2}}^{\eta_{2k}}\frac{w(\eta)}{\eta-\xi}l_i(\eta)\,\mathrm{d}\eta\right]\right\} \\ & +\sum_{k=1}^{n}\left\{\sum_{i=2k-2}^{2k}\hat{\boldsymbol{K}}(\eta_i,\xi)\left[\int_{\eta_{2k-2}}^{\eta_{2k}}w(\eta)l_i(\eta)\,\mathrm{d}\eta\right]\right\}, \\ \boldsymbol{A} = & \sum_{k=1}^{n}\left\{\sum_{i=2k-2}^{2k}\hat{\boldsymbol{\beta}}(\eta_i)\left[\int_{\eta_{2k-2}}^{\eta_{2k}}w(\eta)l_i(\eta)\,\mathrm{d}\eta\right]\right\}. \end{aligned} \tag{A.5}$$

After integration, we can obtain

$$\begin{aligned} f(\xi) = & -\frac{\boldsymbol{L}}{2\pi}\sum_{k=1}^{n}\{E_k(\xi)\hat{\boldsymbol{\beta}}(\eta_{2k-2}) + F_k(\xi)\hat{\boldsymbol{\beta}}(\eta_{2k-1}) + G_k(\xi)\hat{\boldsymbol{\beta}}(\eta_{2k})\} \\ & +\sum_{k=1}^{n}\{a_k\hat{\boldsymbol{K}}(\eta_{2k-2},\xi)\hat{\boldsymbol{\beta}}(\eta_{2k-2}) \\ & \qquad + b_k\hat{\boldsymbol{K}}(\eta_{2k-1},\xi)\hat{\boldsymbol{\beta}}(\eta_{2k-1}) + c_k\hat{\boldsymbol{K}}(\eta_{2k},\xi)\hat{\boldsymbol{\beta}}(\eta_{2k})\}, \end{aligned} \tag{A.6a}$$

$$\boldsymbol{A} = \sum_{k=1}^{n}\{a_k\hat{\boldsymbol{\beta}}(\eta_{2k-2}) + b_k\hat{\boldsymbol{\beta}}(\eta_{2k-1}) + c_k\hat{\boldsymbol{\beta}}(\eta_{2k})\},$$

where

$$\begin{aligned} E_k(\xi) &= \int_{\eta_{2k-2}}^{\eta_{2k}}\frac{w(\eta)}{\eta-\xi}l_{2k-2}(\eta)\,\mathrm{d}\eta = \frac{M(\eta_{2k},\eta_{2k-1})}{(\eta_{2k-2}-\eta_{2k-1})(\eta_{2k-2}-\eta_{2k})}, \\ F_k(\xi) &= \int_{\eta_{2k-2}}^{\eta_{2k}}\frac{w(\eta)}{\eta-\xi}l_{2k-1}(\eta)\,\mathrm{d}\eta = \frac{M(\eta_{2k},\eta_{2k-1})}{(\eta_{2k-1}-\eta_{2k-2})(\eta_{2k-1}-\eta_{2k})}, \\ G_k(\xi) &= \int_{\eta_{2k-2}}^{\eta_{2k}}\frac{w(\eta)}{\eta-\xi}l_{2k}(\eta)\,\mathrm{d}\eta = \frac{M(\eta_{2k-1},\eta_{2k-2})}{(\eta_{2k}-\eta_{2k-2})(\eta_{2k}-\eta_{2k-1})}, \\ a_k(\xi) &= \int_{\eta_{2k-2}}^{\eta_{2k}}w(\eta)l_{2k-2}(\eta)\,\mathrm{d}\eta = \frac{H(\eta_{2k},\eta_{2k-1})}{(\eta_{2k-2}-\eta_{2k-1})(\eta_{2k-2}-\eta_{2k})}, \\ b_k(\xi) &= \int_{\eta_{2k-2}}^{\eta_{2k}}w(\eta)l_{2k-1}(\eta)\,\mathrm{d}\eta = \frac{H(\eta_{2k},\eta_{2k-2})}{(\eta_{2k-1}-\eta_{2k-2})(\eta_{2k-1}-\eta_{2k})}, \\ c_k(\xi) &= \int_{\eta_{2k-2}}^{\eta_{2k}}w(\eta)l_{2k}(\eta)\,\mathrm{d}\eta = \frac{H(\eta_{2k-1},\eta_{2k-2})}{(\eta_{2k}-\eta_{2k-2})(\eta_{2k}-\eta_{2k-1})}, \end{aligned} \tag{A.6b}$$

and

$$
\begin{aligned}
M(x,y) &= \int_{\eta_{2k-2}}^{\eta_{2k}} \frac{w(\eta)}{\eta-\xi}(\eta-x)(\eta-y)\,\mathrm{d}\eta \\
&= \sqrt{1-\eta_{2k-2}^2}-\sqrt{1-\eta_{2k}^2} \\
&\quad +(\xi-x-y)(\theta_{2k}-\theta_{2k-2})+(\xi-x)(\xi-y)A_k(\xi), \\
H(x,y) &= \int_{\eta_{2k-2}}^{\eta_{2k}} w(\eta)(\eta-x)(\eta-y)\,\mathrm{d}\eta \\
&= (\tfrac{1}{2}+xy)(\theta_{2k}-\theta_{2k-2})+(x+y)(\cos\theta_{2k}-\cos\theta_{2k-2}) \\
&\quad +\tfrac{1}{4}(\sin 2\theta_{2k}-\sin 2\theta_{2k-2}), \\
A_k(\xi) &= \int_{\eta_{2k-2}}^{\eta_{2k}} \frac{1}{\sin\theta-\xi}\,\mathrm{d}\theta \\
&= \frac{1}{\sqrt{1-\xi^2}}\log\left|\frac{(-1+\sqrt{1-\xi^2}+\xi\tau_k)\tau_{k-1}+\xi-(1+\sqrt{1-\xi^2})\tau_k}{(-1-\sqrt{1-\xi^2}+\xi\tau_k)\tau_{k-1}+\xi-(1-\sqrt{1-\xi^2})\tau_k}\right|.
\end{aligned}
\tag{A.6c}
$$

$\theta=\sin^{-1}\eta, \tau_k=\tan(\frac{\theta_{2k}}{2})$ for all k. Equation (A.6a) can be reduced to

$$
\begin{aligned}
&-\frac{L}{2\pi}\sum_{i=0}^{2n}\{W_i(\xi)\hat{\beta}(\eta_i)-2\pi V_i L^{-1}\hat{K}(\eta_i,\xi)\hat{\beta}(\eta_i)\}=f(\xi) \\
&\sum_{i=0}^{2n}V_i\hat{\beta}(\eta_i)=A,
\end{aligned}
\tag{A.7a}
$$

where

$$
\begin{aligned}
&V_0=a_1, \qquad V_{2n}=c_n, \\
&V_i=[c_{\frac{i}{2}}+a_{\frac{i+2}{2}}]\delta_{0,\mathrm{mod}(i,2)}+b_{\frac{i+1}{2}}\delta_{1,\mathrm{mod}(i,2)}, \quad i=1,2,\ldots,2n-1, \\
&W_0(\xi)=E_1(\xi), \qquad W_{2n}(\xi)=G_n(\xi), \\
&W_i(\xi)=[G_{\frac{i}{2}}(\xi)+E_{\frac{i+2}{2}}(\xi)]\delta_{0,\mathrm{mod}(i,2)}+F_{\frac{i+1}{2}}(\xi)\delta_{1,\mathrm{mod}(i,2)}, \quad i=1,2,\ldots,2n-1.
\end{aligned}
\tag{A.7b}
$$

$\delta_{i,j}$ is Kronecker delta. Let us choose $2n$ collocation point ξ_k for which $\eta_k \leqslant \xi_k \leqslant \eta_{k+1}, k=0,1,\ldots,2n-1$. Then we obtain $(2n+1)$ linear equations from (A.7a) as

$$
\begin{aligned}
&-\frac{L}{2\pi}\sum_{i=0}^{2n}\{W_i(\xi_k)\hat{\beta}(\eta_i)-2\pi V_i L^{-1}\hat{K}(\eta_i,\xi_k)\hat{\beta}(\eta_i)\}=f(\xi_k) \quad k=0,1,\ldots,2n-1, \\
&\sum_{i=0}^{2n}V_i\hat{\beta}(\eta_i)=A.
\end{aligned}
\tag{A.8}
$$

Solving the $(2n+1)$ equations and applying (A.3), we can obtain the value of the unknown dislocation density function $\beta(\eta)$ at $\eta=\eta_i$, $i=0,\ldots,2n$.

Acknowledgement

The authors would like to thank the National Science Council, Republic of China, for their support through Grant No. NSC 84-2212-E006-026.

References

1. C. Atkinson, *International Journal of Engineering Science* 10 (1972) 127–136.
2. F. Erdogan, G.D. Gupta and M. Ratwani, *Journal of Applied Mechanics* 41 (1974) 1007–1013.
3. F. Erdogan and G.D. Gupta, *International Journal of Fracture* 11 (1975) 13–27.
4. E.M. Patton and M.H. Santare, *International Journal of Fracture* 46 (1990) 71–79.
5. A.H. England, *Journal of Applied Mechanics* 33 (1966) 637–640.
6. M. Toya, *Journal of the Mechanics and Physics of Solids* 22 (1974) 325–348.
7. M. Toya, *International Journal of Fracture* 9 (1973) 463–470.
8. J.M. Herrmann, *International Journal of Solids and Structures* 28 (1991) 1023–1039.
9. G.C. Sih, P.C. Paris and F. Erdogan, *Journal of Applied Mechanics* 29 (1962) 306–312.
10. B. Cotterell and J.R. Rice, *International Journal of Fracture* 16 (1980) 155–169.
11. C. Hwu and C.Y. Liao, *Computers and Structures* 51 (1994) 23–31.
12. W.J. Yen, C. Hwu and Y.K. Liang, *Journal of Applied Mechanics* 62 (1995) 306–311.
13. A. Gerasoulis, *Computational Mathematics with Applications* 8 (1982) 15–22.
14. C. Hwu, *International Journal of Solids and Structures* 30 (1993) 301–312.
15. C. Hwu and T.C.T Ting, *Quarterly Journal of Mechanics and Applied Mathematics* 42 (1989) 553–572.
16. C. Hwu and W.J. Yen, *Journal of Applied Mechanics* 60 (1993) 626–632.
17. C. Hwu and W.J. Yen, *International Journal of Solids and Structures* 27 (1991) 1705–1719.
18. C. Hwu, C.J. Kao and L.E. Chang, *Journal of Composite Materials* (1995) in press.
19. C. Hwu, *International Journal of Fracture* 52 (1991) 239–256.
20. A.H. England, *Complex Variable Method in Elasticity*, John Wiley and Sons Ltd. (1971)
21. A.B. Perlman and G.C. Sih, *International Journal of Engineering Science* 5 (1967) 845–867.